JVSTA Journal of Vacuum Science & Technology A

Surface modification of nitrogen-doped carbon nanotubes by ozone via atomic layer deposition

Andrew Lushington, Jian Liu, Yongji Tang, Ruying Li, and Xueliang Sun

Citation: Journal of Vacuum Science & Technology A **32**, 01A124 (2014); doi: 10.1116/1.4847995
View online: http://dx.doi.org/10.1116/1.4847995
View Table of Contents: http://scitation.aip.org/content/avs/journal/jvsta/32/1?ver=pdfcov
Published by the AVS: Science & Technology of Materials, Interfaces, and Processing

Surface modification of nitrogen-doped carbon nanotubes by ozone via atomic layer deposition

Andrew Lushington, Jian Liu, Yongji Tang, Ruying Li, and Xueliang Sun[a)]
Department of Mechanical and Materials Engineering, University of Western Ontario, London, Ontario N6A 5B9, Canada

(Received 4 September 2013; accepted 2 December 2013; published 17 December 2013)

The use of ozone as an oxidizing agent for atomic layer deposition (ALD) processes is rapidly growing due to its strong oxidizing capabilities. However, the effect of ozone on nanostructured substrates such as nitrogen-doped multiwalled carbon nanotubes (NCNTs) and pristine multiwalled carbon nanotubes (PCNTs) are not very well understood and may provide an avenue toward functionalizing the carbon nanotube surface prior to deposition. The effects of ALD ozone treatment on NCNTs and PCNTs using 10 wt. % ozone at temperatures of 150, 250, and 300 °C are studied. The effect of ozone pulse time and ALD cycle number on NCNTs and PCNTs was also investigated. Morphological changes to the substrate were observed by scanning electron microscopy and high resolution transmission electron microscopy. Brunauer-Emmett-Teller measurements were also conducted to determine surface area, pore size, and pore size distribution following ozone treatment. The graphitic nature of both NCNTs and PCNTs was determined using Raman analysis while x-ray photoelectron spectroscopy (XPS) was employed to probe the chemical nature of NCNTs. It was found that O_3 attack occurs preferentially to the outermost geometric surface of NCNTs. Our research also revealed that the deleterious effects of ozone are found only on NCNTs while little or no damage occurs on PCNTs. Furthermore, XPS analysis indicated that ALD ozone treatment on NCNTs, at elevated temperatures, results in loss of nitrogen content. Our studies demonstrate that ALD ozone treatment is an effective avenue toward creating low nitrogen content, defect rich substrates for use in electrochemical applications and ALD of various metal/metal oxides. © *2014 American Vacuum Society*. [http://dx.doi.org/10.1116/1.4847995]

I. INTRODUCTION

Since the discovery of carbon nanotubes (CNTs) in 1991,[1] their remarkable electronic and mechanical properties have attracted a great deal of attention. The potential applications of CNTs include: sensors, field emission displays, use in hydrogen storage media, and nanosized semiconductor devices, probes, and interconnects.[2] Furthermore, CNTs intrinsically have a high electronic conductivity and large accessible surface area, making them attractive candidates for electrochemical devices.[3] In order to enhance their performance, broaden their properties and expand their applications, various chemical and physical approaches have been pursued to modify the surface of CNTs. Due to the inert and hydrophobic nature of CNTs, surface modification and functionalization is essential for their application. For example, recent studies have shown that the surface modification techniques of CNTs result in the enhancement of lithium storage by allowing access to the inner regions of the tubes via defects and edge formation sites.[4]

Many types of surface modification techniques are employed on CNTs including: mechanical griding,[5] electron irradiation,[6] covalent bonding of functional groups,[7] and noncovalent wrapping or adsorption of mediating molecules onto the carbon nanotube (CNT) surface.[8] Among various surface modification techniques, the bonding of oxygen-containing functional groups to the side walls of CNTs is a popular and versatile approch.[9] Deliberate incorporation of surface oxygen onto CNTs has been achieved through a variety of techniques including chemical oxidation,[10] plasma treatment,[11] and functionalization using synthetic organic chemistry.[12] Chemical oxidation is widely used due to its uniform contact and even distribution of defect density. However, wet chemical oxidation techniques typically use strongly oxidizing chemicals and ultimately lead to tube deterioration and impurities.[10] Gas phase oxidation of CNTs can also be used to create defects and functional groups with the use of oxidizing gasses such as ozone. Gas phase ozonolysis of CNTs has been previously shown to create better adhesion and compatibility with polar surfaces as well as improve dispersion and reactivity with polymeric matrices or solvents.[13] Smalley *et al.*[14] reported the oxidation and etching of CNTs using O_3 at room temperature and demonstrated that the geometrically strained curvature of CNTs resulted in ozone having a high reactivity toward conjugated carbon double bonds. Other studies have also shown that ozonolysis of CNTs results in the shortening of tubes as a result of the oxidation process.[15]

Another method toward the surface modification of CNTs is the doping of heteroatoms such as nitrogen,[16] phosphorus,[17] and boron[18] into the CNT matrix. This method has resulted in improved physical and electrochemical properties of CNTs.[19–22] Nitrogen-doped CNTs (NCNTs) have been shown to be more chemically active than CNTs due to increased surface defects introduced by nitrogen doping.[23] NCNTs have also been shown to have a profound effect on oxygen reduction reaction activity as well as enhanced catalytic splitting of water.[24,25] Furthermore, NCNTs with low

a)Electronic mail: xsun@eng.uwo.ca

nitrogen content have displayed decreased charge-transfer resistance with enhanced electrochemical activity, attributed to the incorporation of graphitic nitrogen atoms.[26]

Both CNTs and NCNTs are seen as attractive candidates for the atomic layer deposition (ALD) processes where thin conformal films can be deposited on high surface area substrates. The ALD of various metal oxides on functionalized CNTs has been shown to greatly improve the performance of supercapacitors,[27] transistors,[28] and field emission devices.[29] However, due to the chemically inert nature of CNTs, ALD deposition on their surface is difficult. For this reason, NCNTs, which have a greater number of active sites, are seen as an attractive candidate for ALD processes. Doped-N atoms have the ability to facilitate or promote the adsorption of precursor molecules in order to initiate the deposition process[30] and have been shown to aid in the ALD of aluminum phosphate,[31] iron oxide,[30] lithium titanium oxide,[32] tin oxide,[33] and zirconium oxide.[34] However, the effect of ozone exposure by ALD on these substrates is not very well understood. Jandhyala *et al.*[35] demonstrated that the use of ozone allows for the functionalization of graphene surfaces and provides a nondestructive way for nucleating growth. The study however did not go into detail as to the amount of ozone exposure required to begin graphene functionalization or how ozone aids in the nucleation process. Given the increasing number of ALD processes that utilize ozone as an oxidizing gas and the attractiveness of CNTs and NCNTs as substrates for ALD, it is imperative to understand the effect ozone may have on these substrates. Furthermore, since the extensive exposure of CNTs to ozone has been previously shown to cause significant destruction, control over exposure conditions and understanding the consequences of ozone oxidation are important parameters to take into account. ALD offers an ideal avenue toward understanding the effect of ozone on these substrates by allowing precise control of ozone exposure in a wide temperature window. In this article, we report the effects ozone has on pristine multiwalled CNTs (PCNTs) and multiwalled NCNTs by ALD. A systematical study was carried out to investigate the effects of temperature, ALD cycle number, and ozone pulse time on the surface modification of PCNTs and NCNTs. Moreover, the working mechanism of ozone on NCNTs was explored and discussed. To the best of our knowledge, this is the first study to thoroughly determine the effect of ALD-ozone on PCNTs and NCNTs and the defects it produces.

II. EXPERIMENT

A. ALD-ozone process

PCNTs were purchased from Shenzhen Nanotech Port Co., Ltd., with a diameter range of 30–150 nm. NCNTs with a diameter range of 20–40 nm were prepared by ultrasonic spray pyrolysis as outlined previously.[26] Both PCNTs and NCNTs were ultrasonicated in ethanol for 20 min and dispersed on aluminum foil for ALD-ozone treatment. Ozone experiments were performed in a commercial ALD reactor (Savannah 100, Cambridge Nanotechnology Inc., USA) using 10% ozone (by weight) generated by an OL80F generator. Nitrogen (99.999%) was selected as the carrier gas with a flow rate of 15 sccm. The ALD reactor was evacuated by a vacuum pump (Pascal 2005 I, Adixon) and reached a base pressure of around 0.7 Torr. Ozone treatment was carried out at a temperature range of 150–300 °C. One cycle of ALD-ozone treatment consisted of the following three steps: (1) a 2 s or 4 s ozone pulse; (2) a 2 s extended exposure of ozone; (3) and a 10 s nitrogen purge to remove residual ozone and possible by-products.

B. Characterization of ozone treated PCNTs and NCNTs

A field-emission scanning electron microscope (Hitachi 4800S) was employed to observe the morphologies of ozone treated PCNTs and NCNTs. In addition, the tube walls of ozone treated NCNTs and CNTs was examined by high-resolution transmission electron microscopy (HRTEM, JEOL 2010 FEG). Raman scattering spectra was recorded on a HORIBA Scientific LabRAM HR Raman spectrometer system equipped with a 532.4 nm laser. X-ray photoelectron spectroscopy (XPS) data were obtained using a Kratos Axis Ultra α unit operating at 14 kV. N_2 adsorption–desorption behavior was monitored using a TriStar II 3020 (Micrometrics, USA) at 77 K. Isotherms were fitted according to the Barett–Joyner–Halenda (BJH) theory to give surface area, pore size, and pore size distribution.

III. RESULTS AND DISCUSSION

SEM images of PCNTs and NCNTs before ozone treatment are shown in Figs. 1(a) and 1(e), respectively. Figure 1(a) displays PCNTs with a wide distribution of diameter between 30 and 150 nm and are tangle and curved in nature with a smooth outer wall surface. Figure 1(e) indicates that the NCNTs are relatively straight and often appear in bundles with a diameter distribution of 20–40 nm.

The reactor temperature was varied from 150 °C to 250 °C and 300 °C, with 500 cycles of ozone. SEM images of PCNTs and NCNTs after ozone exposure at 150 °C, shown in Figs. 1(b) and 1(f), respectively, demonstrate that no morphological changes are observed. Increasing the reactor temperature to 250 °C results in no visible destruction on PCNTs [Fig. 1(c)], while for NCNTs, jagged holes are seen along the basal plane, as presented in Fig. 1(g). The holes are unevenly distributed and range in diameter from a few nanometers up to 30 nm. Furthermore, the number of holes varies from tube to tube. Apart from the visible appearance of surface defects, small agglomerations of material are observed on the outer surface of the NCNTs. Elevating the temperature to 300 °C results in PCNTs maintaining their initial morphology [Fig. 1(d)]. However, Fig. 1(h) clearly indicates that NCNTs undergo significant destruction and lose majority of their tubular nature. In addition, there is a substantial increase in agglomerated material found on the surface of NCNTs. Similar to results for ozone treatment of NCNTs at 250 °C, the level of destruction is not uniform and varies from one tube to another. From the above results, it is clear that ozone treatment at 250 °C and 300 °C results in significant destruction to NCNTs but not to PCNTs. Since

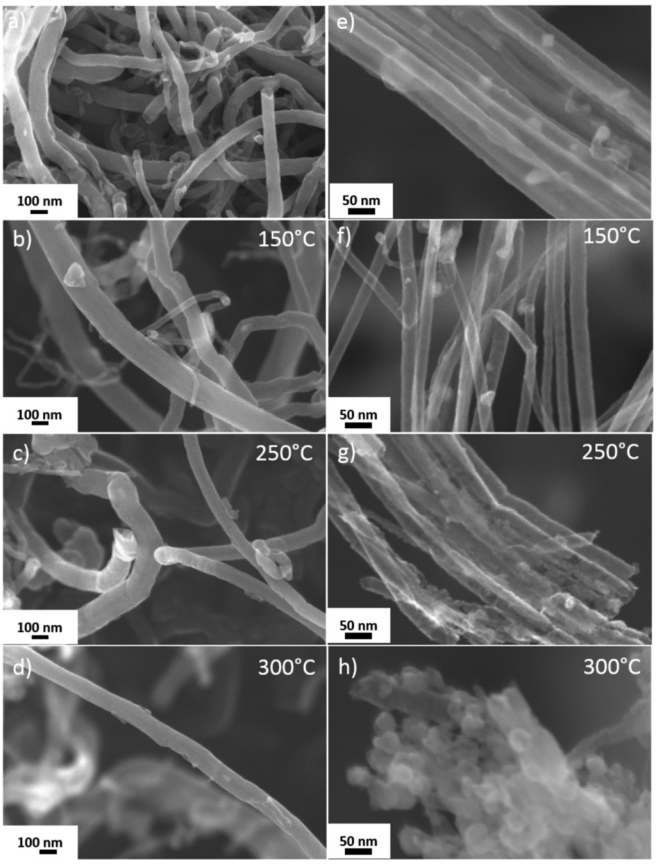

FIG. 1. SEM images of (a) PCNTs and (e) NCNTs before ozone treatment; (b)–(d) PCNTs and (f)–(h) NCNTs after ozone treatment at different temperatures for 500 cycles.

nitrogen doping is a major difference between these two materials, it is reasonable to speculate that nitrogen content plays a significant role in the destruction of NCNT surface.

Armed with the understanding that a reaction between ozone and NCNT surface begins at 250 °C, analysis toward the amount of ozone exposure required to cause destruction was undertaken. ALD provides two unique ways to control ozone exposure, varying number of ALD cycles and controlling ozone pulse length. Figure 2 displays SEM images of NCNTs after ozone treatment with either 2 s or 4 s pulse with varying cycle number at a temperature of 250 °C. Using a 2 or 4 s pulse of ozone for 250 cycles fails to create any visible holes or defects, as indicated in Figs. 2(a) and 2(d). Increasing to 500 cycles, destruction of NCNTs is observed at both 2 s and 4 s ozone pulse lengths and can be seen in Figs. 2(b) and 2(e), respectively. The destruction of NCNTs occurs to a much larger extent using 4 s pulse length than using 2 s. Figure 2(e) also indicates that a 4 s 500-cycle ozone treatment results in the removal of large pieces of NCNTs outer wall surface; however, the tubular structure remains intact. Increasing the number of ALD cycles to 1000 results in the formation of large carbon nanoparticles, as shown in Figs. 2(c) and 2(f). The level of destruction from a 4 s pulse of ozone at 1000 cycles results in greater destruction to the NCNTs, than a 2 s pulse. The appearance of such large carbon particles is a clear indication that 1000 ALD cycles of ozone has a significant effect on NCNTs. The above results suggest that ozone exposure time plays a role in the surface modification of NCNTs.

TEM was employed to gain a more detailed picture as to the structure of NCNTs before and after ozone treatment. As shown in Fig. 3(a), the original NCNTs exhibit a bamboolike structure with a smooth outer wall. However, Fig. 3(b) demonstrates that following ozone treatment at 150 °C, small agglomerated carbonaceous material covers the NCNT surface. Increasing the reactor temperature to 250 °C leads to the formation of much larger agglomerated carbonaceous material accompanied by partial destruction to the outer walls. Black circles shown in Fig. 3(c) highlight the regions where damage to NCNTs occurs. The majority NCNTs retain their tubular nature but lose their branching bamboo element. Based on SEM and TEM results, it can be concluded that ozone treatment not only creates holes on

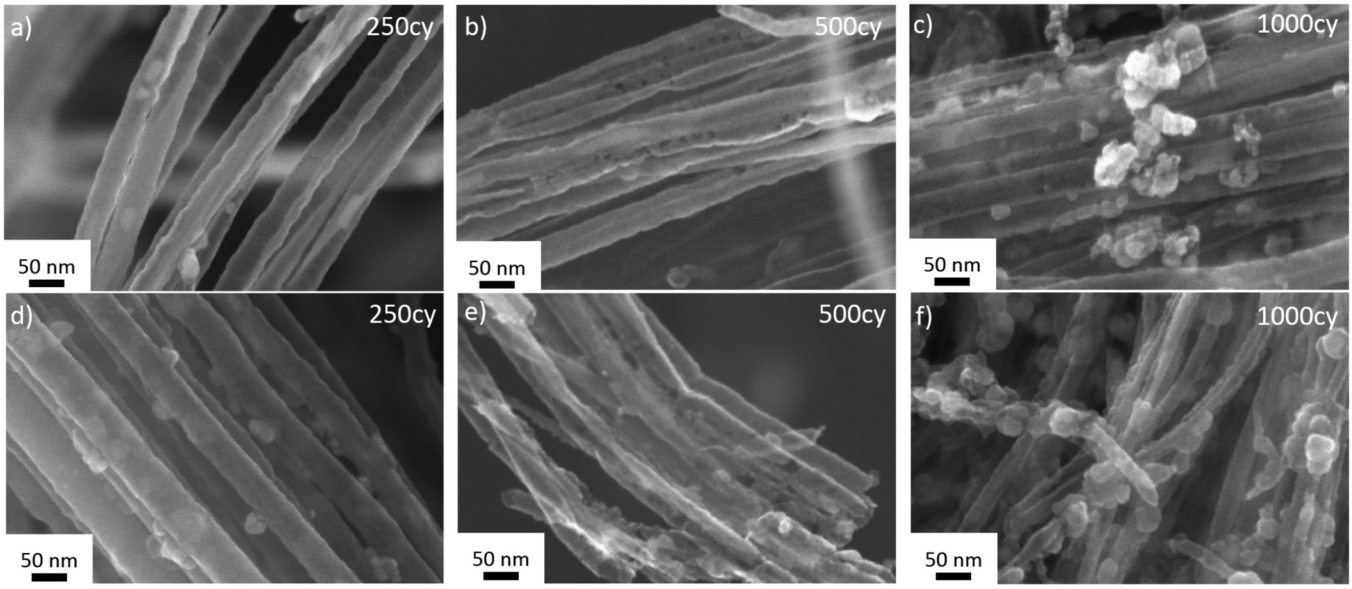

FIG. 2. SEM images of NCNTs treated with (a)–(c) 2 s of ozone pulse and (d)–(f) 4 s of ozone pulse using different cycles at 250 °C.

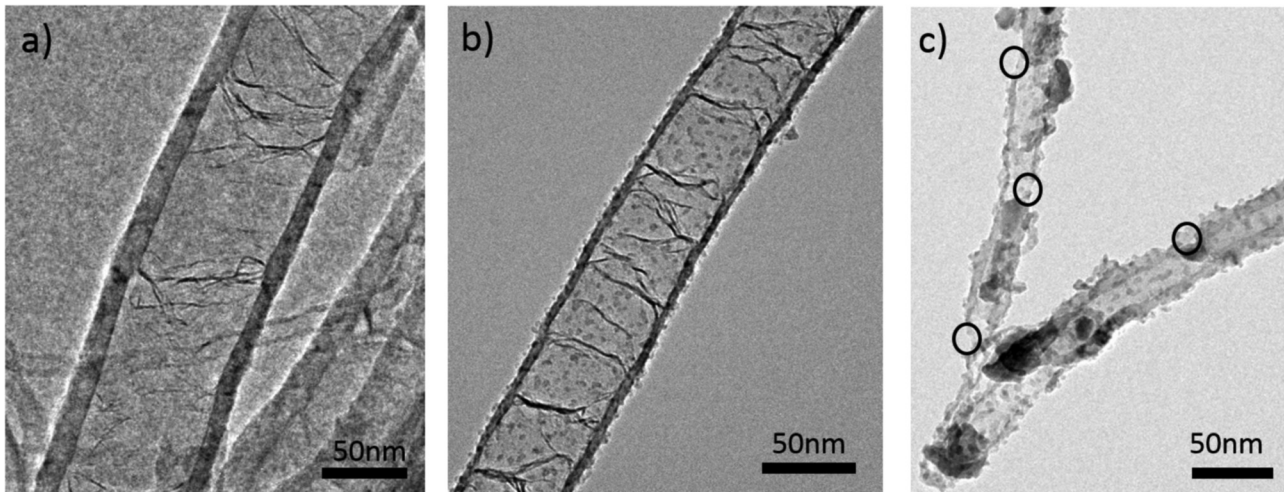

FIG. 3. TEM images (a) untreated NCNTs, ozone treated NCNTs at (b) 150 °C and (c) 250 °C for 500 cycles.

NCNTs but also leads to the formation of spherical carbonaceous material and loss of bamboo structure. These results further prove that nitrogen content plays a critical role in the surface modification of CNTs.

Raman spectroscopy was employed to determine the effect of ozone treatment on the structural ordering in NCNTs. Figure 4(a) presents raw Raman data collected for NCNTs and displays two prominent peaks at 1350 cm^{-1} and 1580 cm^{-1}. The peak occurring at 1350 cm^{-1} is typically a representation toward the amount of disorder within the graphitic plane, commonly referred to as the D band, while the peak at 1580 cm^{-1} reflects well-graphitized carbons in NCNTs, and is referred to as the G band.[36] The data collected indicate an increase in the D-band intensity with elevating reactor temperature while G band intensity decreases. Similar to SEM results, Raman data collected for ozone treated PCNTs at different temperatures (supporting information[37]) Fig. 3 indicate that no significant alterations to the graphitic plane exist. The ratio of intensity between the D band and G band, also know known as I_D/I_G, was used to quantify the graphitic nature of NCNTs.[38,39] Figure 4(b) shows a plot of I_D/I_G versus reactor temperature for NCNTs along with cycle number and pulse time. It can be seen that the I_D/I_G ratio increases from 1.52 to 1.72 when reaction temperature increases from 150 °C to 250 °C. One possible reason for this increase is the formation of carbon nanoparticles on the surface of NCNTs, as previously indicated by Figs. 3(b) and 3(c). This increase in the D band correlates well with SEM and TEM data and provides further evidence that physical defects are introduced at a reactor temperature of 250 °C. Furthermore, the information presented provides strong evidence that an activation barrier may exist between 150 °C and 250 °C and causes ozone to react with nitrogen doping elements that exist in NCNTs. The information presented for pulse length and cycle number versus I_D/I_G ratio in the same graph is also in good agreement with SEM and TEM images. Raman data indicates that at 250 cycles of ozone exposure there is a slight increase in the I_D/I_G ratio and continues to increase with 500 cycles. As expected, the I_D/I_G ratio for 4 s ozone pulse times is consistently higher

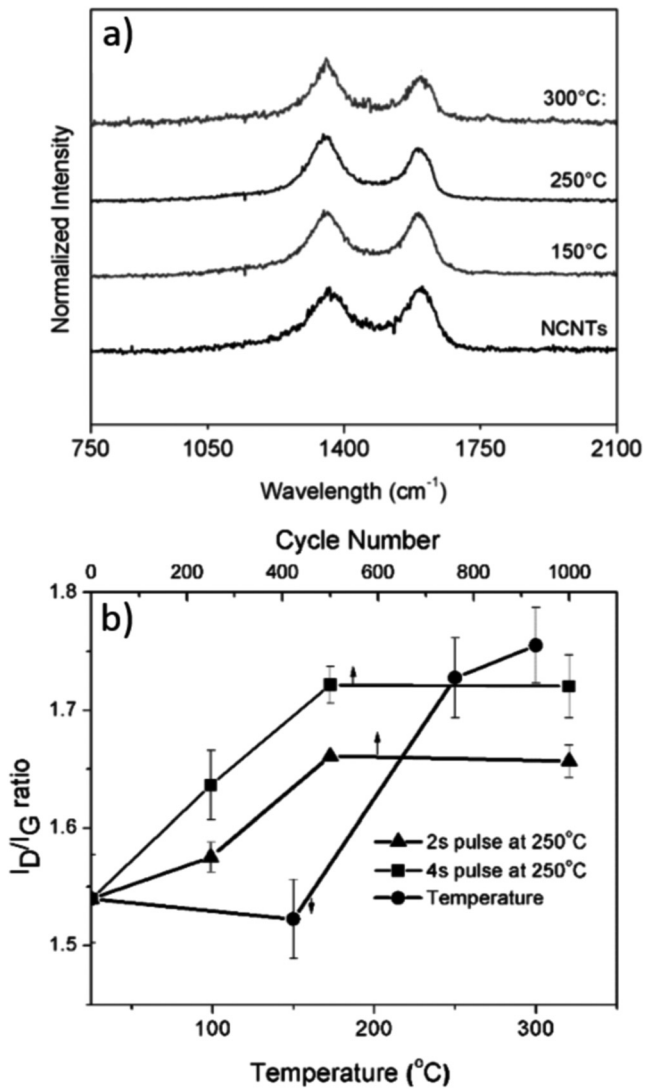

FIG. 4. Raman spectra of (a) NCNTs and before and after ozone treatment at different temperatures; (b) Comparison of I_D/I_G ratio for NCNTs at different temperatures, ALD cycles, and ozone pulse time.

than at a 2 s one. Interestingly, this is also the case for PCNTs, indicating that a 4 s ozone pulse time does causes some interaction to occur on the PCNTs surface, while a 2 s ozone pulse does not, regardless of ALD cycle number (supporting information[37] Fig. 3).

SEM, TEM, and Raman data all provide clear evidence that ozone begins to cause damage to NCNTs at a temperature of 150 °C; however, the mechanism of damage remains unclear. HRTEM was employed in order to gain a better understanding toward the ozone mechanism. As outlined in Fig. 5, HRTEM reveals the extent of damage NCNTs undergo at various temperatures.

Figure 5(a) indicates that untreated NCNTs have an evenly distributed outer wall with a branching element from the inner wall, representing the bamboo structure of NCNTs introduced by nitrogen heteroatom doping. Figure 5(b) shows an HRTEM image of NCNTs treated with ozone at 150 °C for 500 cycles. During treatment at this temperature, short tears to the outer wall begin to appear, as indicated by black arrows. Although the tears are miniscule, they appear only for the first few layers. Formation of amorphous carbon nanoparticles can also be seen as indicated by white arrows in Fig. 5(b). Interestingly, the amorphous carbon nanoparticles appear to be rolled up components of the outer wall. Figures 5(c) and 5(d) are HRTEM images of ozone-treated NCNTs at 250 °C for 500 cycles and indicate that ozone has destroyed the majority of the NCNT wall. Furthermore, this temperature also leads to the exfoliation of NCNT wall. HRTEM images reveals that the number of outer walls for NCNTs treated at 250 °C is dramatically reduced and extremely disordered compared to the untreated NCNTs and NCNTs treated at 150 °C. Black circles in Figs. 5(c) and 5(d) highlight sections that have been completely removed by ALD ozone treatment. Interestingly, the typical inward branching seen for NCNTs is sparsely found in Figs. 5(c) and 5(d). Inward branching of NCNT wall is a result of heteroatom doping, and the loss of this component gives indication that ozone treatment may result in loss of nitrogen content. This would also explain the nonuniform destruction seen across NCNT surface as nitrogen content varies along the tube. Based on SEM, TEM, Raman, and HRTEM results, we can conclude that ozone treatment on NCNTs peel off the outer walls, resulting in the formation of holes. The level of ozone destruction on NCNTs can be controlled by varying reactor temperature, ozone pulse length, and cycle number. However, number of ALD cycles and pulse time also contribute to NCNT destruction, indicating that exposure is a crucial factor toward the surface modification of NCNTs. Furthermore, ozone destruction of NCNTs works by exfoliating and peeling away the outer walls of the NCNT, resulting in the formation of amorphous carbon nanoparticles and the creation of holes on the NCNT surface.

The pore characteristics of as produced NCNTs and 1000 cycle 300 °C ozone treated NCNTs was investigated by nitrogen adsorption isotherms at 77 K. The nitrogen adsorption–desorption isotherms [Fig. 6(a)] indicate that as produced NCNTs and ozone treated NCNTs are both type IV isotherms with pores in the 1.5–100 nm range. However, ozone treated samples reveal a larger presence of mesopores compared to pristine NCNTs. Ozone treated NCNTs also indicated a higher Brunauer-Emmett-Teller surface area of 183.3 m^2/g compared to pristine NCNTs (92.7 m^2/g). Pore size distribution of both samples was determined by the BJH equation [Fig. 6(b)] and indicated that ozone treated samples have a greater volume of pores in the 10–30 nm range. These results correlate well with SEM, TEM, and HRTEM observations and indicate that ozone treatment of NCNTs produces nanosized holes along with a substantial increase in surface area.

XPS analysis was conducted to determine the role of nitrogen doping during ozone treatment of NCNTs. Table I outlines the atomic percentages obtained from an XPS survey spectrum (Fig. 1 of the supporting information[37]) of NCNTs before and after ozone treatment at 300 °C for 500 cycles using a 4 s pulse.

The XPS data reveal that following ozone treatment, NCNTs are comprised of more oxygen but have decreased nitrogen and carbon content. This indicates that not only does ozone etch away the NCNTs surface, but it also causes significant changes to its chemical composition. As a result of ozone treatment, the increase in oxygen content can be ascribed to the introduction of surface hydroxyl, carbonyl, or epoxide functional groups.[40] The decrease in carbon content is due to the removal of carbon layers by ozone treatment as indicated by HRTEM images.

The XPS survey analysis also reveals that binding energies for O1s, N1s, and C1s are lower for ozone-treated

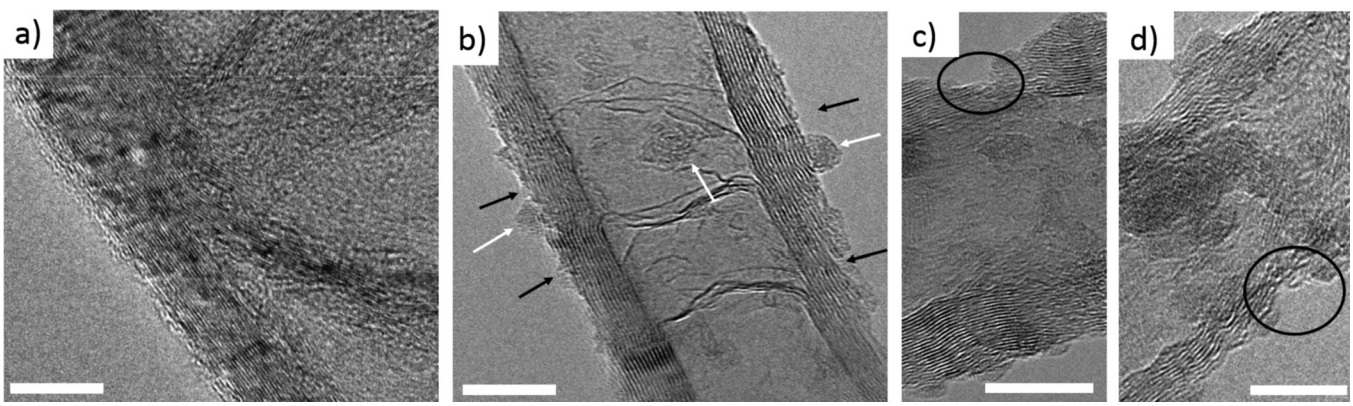

FIG. 5. HRTEM image (a) untreated NCNTs, and ozone treated NCNTs at (b) 150 °C, (c), (d) 250 °C. Scale bar in white represents 10 nm.

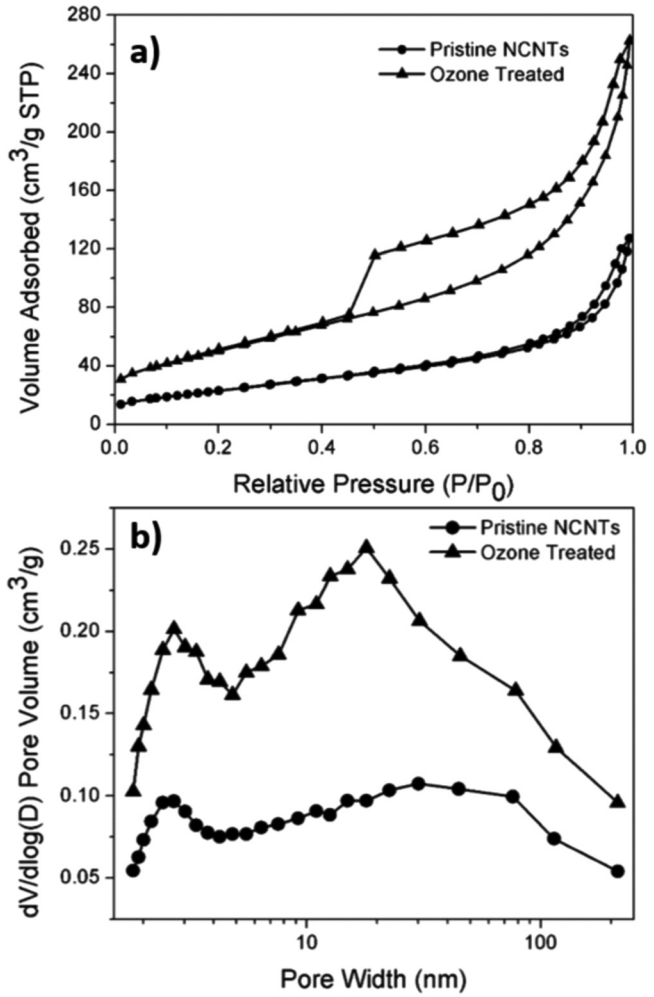

FIG. 6. (a) N_2 adsorption–desorption isotherms at 77 K and (b) pore size distribution of as produced NCNTs and 300 °C ozone treated carbon NCNTs.

NCNTs than untreated NCNTs. Typically, nitrogen doping into CNTs results in a charge transfer to occur between the less electronegative carbon to the more electronegative nitrogen.[41] In NCNTs some homopolar C-C bonds are replaced with heteropolar C-N bonds, resulting in a shift to the C1s core level toward higher binding energies.[42] If less heteropolar C-N bonds exist, the C1s core level binding energy should decrease back toward C-C homopolar bonds, as shown by presented XPS data. A negative shift in the C1s peak may also be ascribed to weaker C-C binding and larger interlayer distance between the CNT walls.[43] From Table I, nitrogen content decreases from 5.1 at. % for as produced NCNTs to 1.8 at. % for ozone-treated NCNTs. High resolution XPS of N1s before and after ozone treatment is displayed in Fig. 7. The N1s peak for untreated NCNTs can be deconvoluted into four peaks located at 398.5, 400.9, 403.5, and 405.1 eV corresponding to pyridinic N, graphitic N, molecular N_2, and chemisorbed N-oxides, respectively.[42] Molecular N_2 has been previously reported to predominantly exist intercalated into the graphite layers of NCNTs.[44] Pyridinic nitrogen species are nitrogen atoms that contribute to the π-system with one p-electron, while graphitic N sits in-plane and replaces a graphitic host carbon atom.[45] For ozone-treated NCNTs, only pyridinic N and graphitic N are observed, indicating a loss in diatomic molecular nitrogen and nitrogen oxide species. Furthermore, ozone treated NCNTs display a decrease in graphitic nitrogen, from 2.0% to 1.0% as well as a slight decrease in pyridinic nitrogen, from 1.3% to 0.8%. Clearly, a relationship exists between nitrogen content and the surface modification of NCNTs. It is also important to distinguish between effects induced by thermal treatment and ozone treatment. Kundu *et al.*[46] conducted a series of experiments toward the stability of various nitrogen species that exists within NCNTs with respect to temperature. They noted that at a temperature of 450 °C, far above the temperatures used in this study, both molecular nitrogen and chemisorbed nitrogen oxide species remain with NCNTs and are detectable by XPS analysis. Clearly the disappearance of these two peaks is related to ALD ozone treatment.

TABLE I. XPS survey analysis comparison between untreated NCNTs and 300 °C ozone treated NCNTs.

	Binding energy (eV)		At. % (±0.1%)	
Element	Untreated	Ozone treated	Untreated	Ozone treated
O1s	531.4	527.9	1.6	14.2
C1s	284.4	280.9	92.7	78.6
N1s	400.6	396.4	5.1	1.8
N1s-Pyridine	398.5	398.8	1.3	0.8
N1s-Graphitic	400.9	400.9	2.0	1.0
N1s-Molecular N_2	403.5	—	0.5	0
N1s-N-oxide	405.1	—	1.3	0

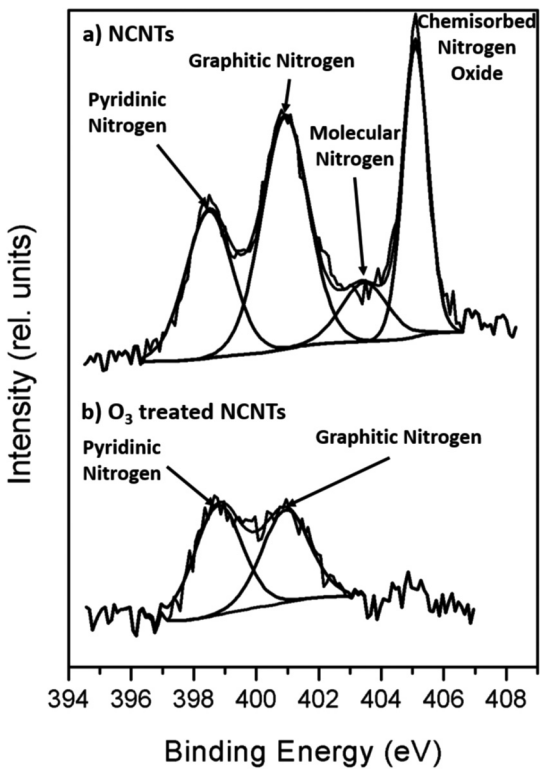

FIG. 7. N1s spectra for NCNTs (a) before ozone treatment and (b) after ozone treatment at 300 °C for 500 cycles.

As mentioned previously, the peak at 403.5 eV is assigned to the incorporation of molecular nitrogen. HRTEM images indicate that following ozone treatment, exfoliation of the graphitic layers occurs. This increase in interlayer distance may result in molecular nitrogen desorbing from between graphitic layers, and resulting in the loss of this peak. Furthermore, the incorporation of holes through the basal plane of the NCNT surface will also allow for adsorbed molecular nitrogen within the tube to escape, especially under the thermal vacuum conditions of ALD. The disappearance of the peak at 405.1 eV (chemisorbed nitrogen oxide groups) is less straightforward and can be related to the decrease in pyridinic and substitution nitrogen also observed. Theoretical calculations have demonstrated that the incorporation of nitrogen atoms into the graphitic framework results in localized high charge density.[47] Nitrogen oxide species have also been shown to contain one negative charge and display nucleophilic ability, resulting in a similar localized charge density.[48] These high charge density sites are preferential locations for initiating oxidation.[49] Furthermore, chemisorbed nitrogen oxide groups are held to the surface by weak dangling bonds and can be easily removed during oxidation.

The use of ozone in an ALD process has been shown to be quite complicated and highly dependent on surface properties. Our results indicate that destruction of NCNTs surface is related to nitrogen content reacting with ozone species. We therefore propose that the uneven destruction seen in SEM, TEM, and HRTEM stem from fluctuating nitrogen content from tube to tube. Knoops *et al.*[50] has demonstrated that depending on the surface, ozone undergoes a recombinative surface loss process via ozone decomposition. The mechanism for O_3 surface loss on MnO_2 proposed by Li *et al.*[51] is considered a standard model for the decomposition pathway on other surfaces and occurs via the following mechanism, where * refers to reactive surface sites:

$$O_3(g) + {}^* \rightarrow O_2(g) + O^*, \quad (1)$$

$$O_3(g) + O^* \rightarrow O_2(g) + O_2{}^*, \quad (2)$$

$$O_2{}^* \rightarrow O_2(g) + {}^*. \quad (3)$$

As mentioned previously, nitrogen sites, particularly pyridinic nitrogen and chemisorbed nitrogen sites, are areas of localized charge densities and are prone to ozone attack. Furthermore, p-type oxides have been shown to demonstrate a high activity for ozone decomposition.[52] This correlates well with recent findings that contrary to the expectation of the n-type doping nature of nitrogen, pyridines-like bonding configurations actually display p-type doping in air.[53] Pyridine nitrogen configuration may then act as a catalyst toward ozone decomposition and cause localized oxidation to occur, resulting in the removal of carbon content. As carbon content is etched away, attached graphitic substituted nitrogen will also be lost. This hypothesis is consistent with XPS data, indicating a substantial loss in graphitic, molecular, and chemisorbed nitrogen, but not pyridinic nitrogen due to its catalytic ability.

IV. SUMMARY AND CONCLUSIONS

We report, for the first time, the effect of ALD ozone on NCNTs and PCNTs. The results indicate that at temperatures of 250 °C and above, ozone has a deleterious effect on the surface of NCNTs, but little or no effect on PCNTs. However, HRTEM results indicate that even at lower reactor temperatures, ozone begins to etch away at the outer wall of NCNTs. Raman measurements on ALD ozone temperature experiments indicate that an activation barrier may exist toward the selective destruction of NCNT outer wall surface. Further experimentation revealed that both pulse time and number of ALD ozone cycles also play an important role in the surface modification of NCNTs. Finally, XPS analysis revealed that ALD ozone treatment results in a decrease in pyridinic and graphitic nitrogen species while a complete loss in molecular and physisorbed nitrogen content is observed. The reaction mechanisms under ALD ozone may be associated with a recombinative process, and depends on ALD conditions as well as reacting surface species. As a result, ALD ozone treatment on NCNT leads to loss in nitrogen content and deterioration of NCNT surface. These results pave the way for understanding the use of ozone during ALD deposition on NCNTs and PCNTs while providing a method for controlling surface defects and composition of carbon nanotubes via a simple ALD process.

ACKNOWLEDGMENTS

This work was supported by the Natural Sciences and Engineering Research Council of Canada (NSERC), Canada Foundation for Innovation (CFI), Canadian Research Chair's (CRC), and the University of Western Ontario.

[1]S. Iijima, Nature **354**, 56 (1991).
[2]R. H. Baughman, A. A. Zakhidov, and W. A. de Heer, Science **297**, 787 (2002).
[3]Z. Xiong, Y. S. Yun, and H. Jin, Materials **6**, 1138 (2013).
[4]H. S. Oktaviano, K. Yamada, and K. Waki, J. Mater. Chem. **22**, 25167 (2012).
[5]Á. Kukovecz, T. Kanyó, Z. Kónya, and I. Kiricsi, Carbon **43**, 994 (2005).
[6]A. Krasheninnikov, K. Nordlund, and J. Keinonen, Phys. Rev. B **65**, 165423 (2002).
[7]K. Balasubramanian and M. Burghard, Small **1**, 180 (2005).
[8]A. Star, Y. Liu, K. Grant, L. Ridvan, J. F. Stoddart, D. W. Steuerman, M. R. Diehl, A. Boukai, and J. R. Heath, Macromolecules **36**, 553 (2003).
[9]K. A. Wepasnick, B. A. Smith, J. L. Bitter, and D. H. Fairbrother, Anal. Bioanal. Chem. **396**, 1003 (2010).
[10]V. Datsyuk, M. Kalyva, K. Papagelis, J. Parthenios, D. Tasis, A. Siokou, I. Kallitsis, and C. Galiotis, Carbon **46**, 833 (2008).
[11]N. P. Zschoerper, V. Katzenmaier, U. Vohrer, M. Haupt, C. Oehr, and T. Hirth, Carbon **47**, 2174 (2009).
[12]A. Gromov, S. Dittmer, J. Svensson, O. A. Nerushev, S. A. Perez-García, L. Licea-Jiménez, R. Rychwalski, and E. E. B. Campbell, J. Mater. Chem. **15**, 3334 (2005).
[13]K. Peng, L. Liu, H. Li, H. Meyer, and Z. Zhang, Carbon **49**, 70 (2011).
[14]D. B. Mawhinney, V. Naumenko, A. Kuznetsova, J. T. Yates, J. Liu, and R. Smalley, J. Am. Chem. Soc. **122**, 2383 (2000).
[15]Z. Chen, K. J. Ziegler, J. Shaver, R. H. Hauge, and R. E. Smalley, J. Phys. Chem. B **110**, 11624 (2006).
[16]H. Liu, Y. Zhang, R. Li, X. Sun, S. Désilets, H. Abou-Rachid, M. Jaidann, and L.-S. Lussier, Carbon **48**, 1498 (2010).
[17]J. Liu, H. Liu, Y. Zhang, R. Li, G. Liang, M. Gauthier, and X. Sun, Carbon **49**, 5014 (2011).
[18]L. Yang *et al.*, Angew Chemie. **123**, 7270 (2011).

[19]C. W. B. Bezerra, L. Zhang, K. Lee, H. Liu, A. L. B. Marques, E. P. Marques, H. Wang, and J. Zhang, Electrochim. Acta **53**, 4937 (2008).
[20]S. Maldonado and K. J. Stevenson, J. Phys. Chem. B **109**, 4707 (2005).
[21]P. H. Matter, E. Wang, M. Arias, E. J. Biddinger, and U. S. Ozkan, J. Phys. Chem. B **110**, 18374 (2006).
[22]F. Charreteur, F. Jaouen, S. Ruggeri, and J. Dodelet, Electrochim. Acta **53**, 2925 (2008).
[23]A. H. Nevidomskyy, G. Csányi, and M. C. Payne, Phys. Rev. Lett. **91**, 105502 (2003).
[24]K. Gong, F. Du, Z. Xia, M. Durstock, and L. Dai, Science **323**, 760 (2009).
[25]X. Wang, K. Maeda, A. Thomas, K. Takanabe, G. Xin, J. M. Carlsson, K. Domen, and M. Antonietti, Nat. Mater. **8**, 76 (2009).
[26]L. G. Bulushevaa, A. V. Okotruba, A. G. Kurenya, Hongkun Zhang, Huijuan Zhang, X. Chen, and H. Song, Carbon **49**, 4013 (2011).
[27]S. Boukhalfa, K. Evanoff, and G. Yushin, Energy Env. Sci. **5**, 6872 (2012).
[28]A. Javey *et al*., Nat. Mater. **1**, 241 (2002).
[29]J. M. Green, L. Dong, T. Gutu, J. Jiao, J. F. Conley, and Y. Ono, J. Appl. Phys. **99**, 094308 (2006).
[30]X. Meng, M. Ionescu, M. N. Banis, Y. Zhong, H. Liu, Y. Zhang, S. Sun, R. Li, and X. Sun, J. Nanopart. Res. **13**, 1207 (2011).
[31]J. Liu, Y. Tang, B. Xiao, T. Sham, R. Li, and X. Sun, RSC Adv. **3**, 4492 (2013).
[32]X. Meng, J. Liu, X. Li, M. N. Banis, J. Yang, R. Li, and X. Sun, RSC Adv. **3**, 7285 (2013).
[33]X. Meng, Y. Zhong, Y. Sun, M. N. Banis, R. Li, and X. Sun, Carbon **49**, 1133 (2011).
[34]J. Liu, X. Meng, M. N. Banis, M. Cai, R. Li, and X. Sun, J. Phys. Chem. C **116**, 14656 (2012).
[35]S. Jandhyala *et al*., ACS Nano **6**, 2722 (2012).
[36]T. Sharifi, F. Nitze, H. R. Barzegar, C.-W. Tai, M. Mazurkiewicz, A. Malolepszy, L. Stobinski, and T. Wågberg, Carbon **50**, 3535 (2012).
[37]See supplementary material at http://dx.doi.org/10.1116/1.4847995 for HRTEM and Raman data for ozone treated PCNTs. Due to relative inertness observed during experimentation, this data was transferred to the supporting information section. Also for additional XPS information such as NCNT survey spectrum as well as high resolution C1s spectrum for untreated and treated NCNTs.
[38]R. Droppa, C. T. M. Ribeiro, A. R. Zanatta, M. C. dos Santos, and F. Alvarez, Phys. Rev. B **69**, 045405 (2004).
[39]S. Osswald, M. Havel, and Y. Gogotsi, J. Raman Spectrosc. **38**, 728 (2007).
[40]M. Sham and J. Kim, Carbon **44**, 768 (2006).
[41]S. H. Lim, H. I. Elim, X. Y. Gao, A. T. S. Wee, W. Ji, J. Y. Lee, and J. Lin, Phys. Rev. B **73**, 45402 (2006).
[42]C. Morant, J. Andrey, P. Prieto, D. Mendiola, J. Sanz, and E. Elizalde, Phys. Status Solidi A **203**, 1069 (2006).
[43]P. Chen, X. Wu, X. Sun, J. Lin, W. Ji, and K. Tan, Phys. Rev. Lett. **82**, 2548 (1999).
[44]H. C. Choi, S. Y. Bae, J. Park, K. Seo, C. Kim, B. Kim, H. J. Song, and H.-J. Shin, Appl. Phys. Lett. **85**, 5742 (2004).
[45]C. Ewels and M. Glerup, J. Nanosci. Nanotechnol. **5**, 1345 (2005).
[46]S. Kundu *et al*., J. Phys. Chem. C **113**, 14302 (2009).
[47]E. Cruz-Silva, F. López-Urías, E. Munoz-Sandoval, B. G. Sumpter, H. Terrones, J.-C. Charlier, V. Meunier, and M. Terrones, ACS Nano **3**, 1913 (2009).
[48]X. Shi, Y. Feng, X. Wang, H. Lee, J. Liu, Y. Qu, W. He, S. M. Kumar, and N. Ren, Bioresour. Technol. **108**, 89 (2012).
[49]R. Cruz-Silva *et al*., ACS Nano **7**, 2192 (2013).
[50]H. C. Knoops, J. W. Elam, J. A. Libera, and W. M. Kessels, Chem. Mater. **23**, 2381 (2011).
[51]W. Li, G. Gibbs, and S. T. Oyama, J. Am. Chem. Soc. **120**, 9041 (1998).
[52]B. Dhandapani and S. T. Oyama, Appl. Catal. B: Env. **11**, 129 (1997).
[53]Y.-S. Min, E. J. Bae, U. J. Kim, E. H. Lee, N. Park, C. S. Hwang, and W. Park, Appl. Phys. Lett. **93**, 43113 (2008).